

# Soft Hybrid Wave Spring Actuators

Erik H. Skorina and Cagdas D. Onal\*

Soft continuum manipulators, inspired by squid tentacles and elephant trunks, show promise in allowing robots to safely interact with complex environments. One ongoing problem for these manipulators is torsional stiffness, as continuum manipulators are naturally compliant and cannot actively resist torsional strain. A hybrid actuator that combines molded silicone actuators with 3D printed flexible wave springs is used to overcome this problem. It is shown that the inclusion of the 3D printed wave spring increases actuator torsional stiffness by up to a factor of 10. Further investigation of these structures is performed using both experimentation and simulation. Finally, this hybrid actuator design is used to create a nine-degree-of-freedom soft continuum manipulator, which is used to perform a cantilevered pick-and-place task impossible for a traditional soft manipulator of similar size.

## 1. Introduction

Due to their weight and rigidity, robots operated by traditional motors can be dangerous to humans, limiting their ability to operate efficiently in human-inhabited environments. Soft actuators can absorb energy to enable safe and compliant physical interaction with the environment in a way that is similar to biological muscles, allowing for a bioinspired approach to robotics and actuation. One important category of soft robots is continuum robots or manipulators. These structures bend continuously along their actuation areas instead of at a discrete axle, similar to elephant trunks, octopus tentacles, or snakes.

An example of soft continuum manipulator is the Octarm,<sup>[1]</sup> which uses McKibben muscles that contract under pressure. Another example was discussed by Gerboni et al.<sup>[2]</sup> Intended for minimally invasive surgery, this work uses cylindrical pressure chambers within a larger cylinder of elastic material constrained by a vascular graft. When pressurized, the graft prevents expansion, resulting in segment extension and bending. Another continuum manipulator was found in Zhang et al.,<sup>[3]</sup> which uses

cables to apply bending and contractile forces to a folded plastic structure. Cables can also be used in conjunction with pneumatics, such as by McMahan et al.<sup>[4]</sup> when they were combined with a pressurized bladder to provide structure.

Low stiffness is often a problem in continuum manipulation.<sup>[4,5]</sup> Easy bending in multiple directions allows continuum manipulators to achieve tortuous configurations, but can make it difficult to interact with the world. One example application, discussed in Loeve et al.,<sup>[6]</sup> is for soft endoscopes, which need to be soft for some places but rigid in others. Much of the work on stiffness in continuum manipulators is focused on changing the omnidirectional stiffness of some or all of a continuum

manipulator.<sup>[7,8]</sup> One method for stiffness control is done by including a granular jamming chamber in the bending segment.<sup>[9]</sup> Another involves using a phase changing alloy, which can be melted to allow manipulator movement or solidified to create a high-strength configuration.<sup>[10]</sup> Sadati et al.<sup>[11]</sup> used 3D printing to insert a helical arrangement of wax within their continuum manipulator, which they can heat or cool to continuously change the stiffness. All these methods allow for high stiffness under load, but do not allow for this stiffness to be maintained at manipulator segments undergoing active motion with full maneuverability.

Some work has been done to create continuum actuators with differing stiffness in different directions. In particular, having a much higher axial torsional stiffness than a longitudinal or bending stiffness is useful because most continuum bending manipulators cannot apply forces in the axial direction. When subjected to an axial torque, most continuum manipulators will undergo a twist that they are unable to actively resist, reducing system performance.<sup>[12]</sup> An example of this deformation is shown in **Figure 1**. Even the most capable continuum manipulators that exist in the literature, such as the Octarm,<sup>[1]</sup> do not discuss torsional stiffness and do not discuss or demonstrate off-axial manipulation.

Works were done by Santoso et al.<sup>[12]</sup> and others<sup>[13]</sup> using origami bellows. We have found that our origami system had a torsional stiffness 160 times than one of the few continuum manipulators that reports their torsional stiffness.<sup>[14]</sup> Fabricating origami structures can be a difficult, laborious process, and can be difficult to scale down.<sup>[15]</sup> Murphy et al.<sup>[16]</sup> used cables to drive a continuum manipulator made of a notched nitinol tube. While the structure appears to have a high torsional stiffness, the authors do not discuss it. Xu et al.<sup>[17]</sup> added rigid joints within their cable-driven continuum manipulator, increasing its stiffness at the cost of a reduction in manipulation capability.

Dr. E. H. Skorina, Prof. C. D. Onal  
WPI Soft Robotics Laboratory  
Mechanical Engineering Department  
Robotics Engineering Program  
100 Institute Rd, Worcester, MA 01609, USA  
E-mail: cdonal@wpi.edu

 The ORCID identification number(s) for the author(s) of this article can be found under <https://doi.org/10.1002/aisy.201900097>.

© 2019 The Authors. Published by WILEY-VCH Verlag GmbH & Co. KGaA, Weinheim. This is an open access article under the terms of the Creative Commons Attribution License, which permits use, distribution and reproduction in any medium, provided the original work is properly cited.

DOI: 10.1002/aisy.201900097

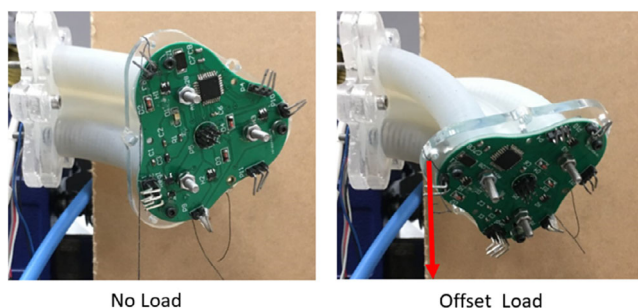


**Figure 1.** An example of a pneumatic continuum manipulator, actuated to bend out of the page, with and without an offset load of 0.68 N. The offset load causes significant actuator torsion, which cannot be resisted by more actuation.

In this work, we discuss a new such paradigm combining 3D printing techniques with traditional pneumatic bending approaches. This approach uses a wave spring printed out of flexible filament that exhibits torsional stiffness while still being capable of extension, retraction, and bending. We used these structures to augment existing fiber-reinforced soft actuators, creating a hybrid actuator. We investigated different materials and configurations before settling on using the flexible wave spring as an external sheath to the underlying actuator, an example of which is shown in **Figure 2**. With this configuration settled on, we investigated the effects of varying the wave spring parameters on segment torsional stiffness. Finally, we created a nine-degree-of-freedom (DoF) soft continuum manipulator and used it to perform a pick-and-place task that would be impossible with a traditional soft manipulator of comparable size.

The existing pneumatic actuator used in this work is the reverse pneumatic artificial muscle (rPAM), a soft linear actuation concept inspired by biological anatomy, which we introduced in 2015<sup>[18]</sup> and have further analyzed.<sup>[19,20]</sup> This actuator is called the rPAM because it operates on similar principles to the traditional PAM (also known as the McKibben actuator<sup>[21]</sup>), only with a reversed direction of actuation (similar to the work of Gaylord et al.<sup>[22]</sup>). Our approach utilizes these fiber-reinforced

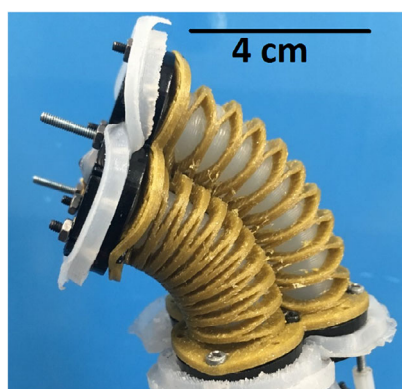


**Figure 2.** The three-chamber wave spring actuator being actuated. The waves of the wave spring serve the role of threading while providing the actuator with torsional stiffness, allowing it to actuate in desired directions while resisting deformation in others.

elastomer tubes either in a prestrained state when driving a rigid kinematic skeleton, or as part of a soft bending continuum manipulator (a segment that bends gradually, and not at along a single axis). We have previously used rPAM actuators to drive rigid joints<sup>[20]</sup> or as part of soft bending segments.<sup>[23]</sup>

3D printing is not a stranger to soft robotic actuators. Several groups have created bending actuators out of soft 3D printed materials, often using bellows configurations.<sup>[24,25]</sup> A wide range of materials has been used, including NinjaFlex<sup>[26]</sup> and mixtures of TangoBlack and VeroClear.<sup>[27]</sup> Mori et al.<sup>[27]</sup> used the complicated structures achievable by 3D printing to incorporate bending sensors. Yirmibesoglu et al.<sup>[28]</sup> used 3D printing to directly print silicone, finding similar performance between printed and molded DragonSkin. Plott et al.<sup>[29]</sup> discussed problems with 3D printing silicone, where voids between extruded layers propagated under high strain, which could be mitigated by different printing patterns.

Work was done combining 3D printing techniques with more traditional soft actuator fabrication techniques. Yuan et al.<sup>[30]</sup> combined 3D printed flexible materials with liquid crystal elastomers to create a range of actively deforming structures. This work used the 3D printed material TangoBlack to provide structure and a restoring force to the actuators.

The contributions of this article are as follows: 1) the creation of a torsional stiffness constraint layer for soft actuators; 2) the creation and characterization of a new hybrid molded/3D printed pneumatic actuator with high torsional stiffness; and 3) the creation and demonstration of a soft, torsionally stiff nine-DoF manipulator.

## 2. Soft Wave Spring Augmented Pneumatic Actuator Verification

The actuators discussed in this article have two main components: the silicone core and the wave spring. The silicone core provides an air-tight pressure chamber to allow the pneumatic actuator to convert air pressure into directed forces. In traditional construction, such as in our previous work, the silicone core includes wrap of constraint thread that prevents it from expanding radially when pressurized, instead causing it to extend linearly. We use twin plates of acrylic on either end of the actuator, sandwiching flanges of silicone, to seal with pressure chamber.

The wave spring serves to provide torsional stiffness to the actuator and is mounted between the ends of the actuator. Because of the thin nature of the wave springs, they were unsuitable for the same molding fabrication process as the silicone cores. We examined the possibility of using commercially available wave springs, but chose to 3D print them ourselves to have greater control over the wave spring parameters. This hybrid fabrication method, combining 3D printing and traditional molding techniques, was chosen because it could take advantage of both the superior elasticity of silicone and the superior geometric complexity allowed by 3D printing. A secondary benefit that the wave springs could bring would be to replace the constrain threading. This would speed up the actuator fabrication process, reducing the necessary steps and eliminating the need for the second layer of silicone to cure. Our initial experiments with

wave spring actuators focus on verifying the properties of wave spring actuators, examining both configuration and material.

### 2.1. Single-Chamber Actuator

We first created and verified the torsional stiffness of the linear wave spring actuators, as shown in **Figure 3a**. We compared two separate ways of including the wave spring in the actuator: internal and external. In external wave springs, the wave spring is used as a sheath, slipping on outside the silicone core. In the internal configuration, wave spring is mounted inside the wall of the actuator. This is done by inserting it into the mold used to form the elastic core before the silicone is poured in. The silicone pressure chamber has an inner diameter of 2 cm and an outer diameter of 3 cm, whereas the wave spring beams are 2.5 mm wide and 1.25 mm tall. A more detailed look at the wave spring parameters is described in Section 3.

We performed torsional stiffness experiments on these two wave spring actuators. These experiments were performed using weights to apply an axial moment to the actuator, with an OptiTrak motion capture system used to measure actuator deformation. More detail about the experimental setup can be found in our previous work.<sup>[12]</sup> The wave springs were printed on an Objet 260 Connex 3D printer using the FLX 9085 mixture of TangoPlus (soft) and VeroClear (rigid). We compared the internal and external wave spring actuators with a control actuator without a wave spring. Torque–Displacement results of these experiments are shown in **Figure 3b**.

From this figure, we can see that the addition of the wave spring dramatically increased the torsional stiffness of the actuator. The internal wave spring actuator was twice as stiff as the control actuator, whereas the external wave spring actuator was six times stiffer than the control actuator. This increase in stiffness of the external wave spring was probably not only because the external wave spring could have a larger diameter but also because the internal wave spring could not be directly anchored to the end caps of the actuator. In addition, the internal wave springs exhibited a series of fabrication difficulties, including difficulties staying properly situated in the mold, whereas the

silicone was curing and the difficulty of preventing pressurized air from seeping into cracks between the silicone and the wave spring. For these reasons, we chose to continue using the external wave spring method.

### 2.2. Three-Chamber Wave Spring Actuators

Maintaining this external configuration, we also adapt this wave spring actuator methodology to three-DoF bending actuators, widely used configuration of soft actuators, with multiple soft pneumatic actuators mounted together. When one of the actuators is pressurized, the entire segment bends appropriately. We combined three wave springs into a single unit, fusing them together at their tangent faces. We also created a three-chamber wave spring using NinjaFlex, a cheaper and more reliable material than FLX 9085. The pressure chamber had inner diameters of 7.5 mm and outer diameters of 13 mm, with the same dimension of wave spring (except the diameter of the wave, which was adjusted to stay in contact with the outer face of the actuators). These three-chamber wave spring actuators are shown in **Figure 4a**, whereas an actuated version is shown in **Figure 2**.

We performed a torsion test using the two three-chamber wave spring actuators and the silicone control using the same methodology as before. The results of these experiments are shown in **Figure 4b**, where we again found that the wave springs increased the torsional stiffness of the bending segment by a factor of 10. We also found a negligible difference between torsional stiffness of the wave spring printed using FLX 9085 and with NinjaFlex.

## 3. Parameter Investigation

We investigated the effect of changing parameters on the torsional stiffness of the one-chamber wave springs. A single, unwrapped, level of the wave spring is shown in **Figure 5a**. We investigated the effects of changing two parameters: the amplitude of the wave and the period of the wave. The amplitude is the distance between the top and bottom of each wave, which

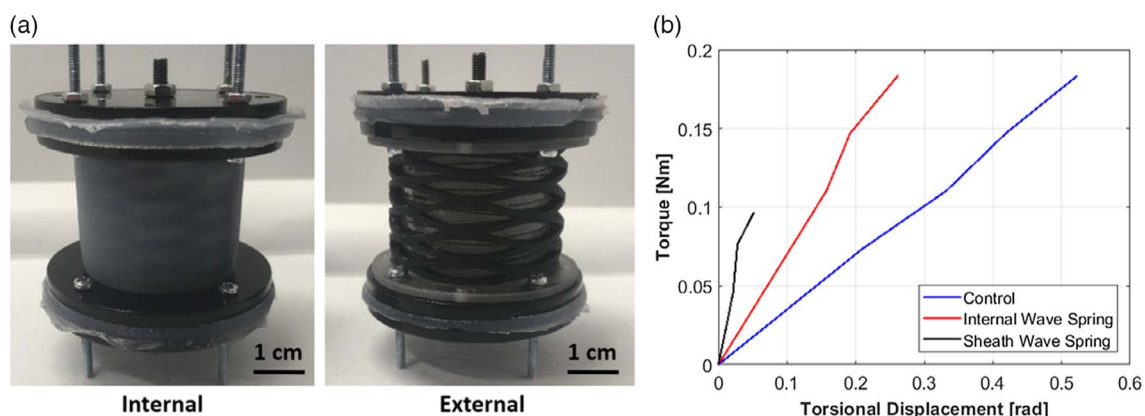


**Figure 3.** a) Two examples of soft, linear wave spring actuators with different placements of the wave spring. Materials used were FLX 9085 for the wave spring and EcoFlex 0030 for the silicone pressure chamber. b) Torsion test results for our single-chamber wave spring actuators. We compared the torsional behavior of the actuator with the wave spring mounted inside the actuator wall with it mounted outside the actuator wall. Materials used were FLX 9085 for the wave spring and EcoFlex 0030 for the silicone pressure chamber.

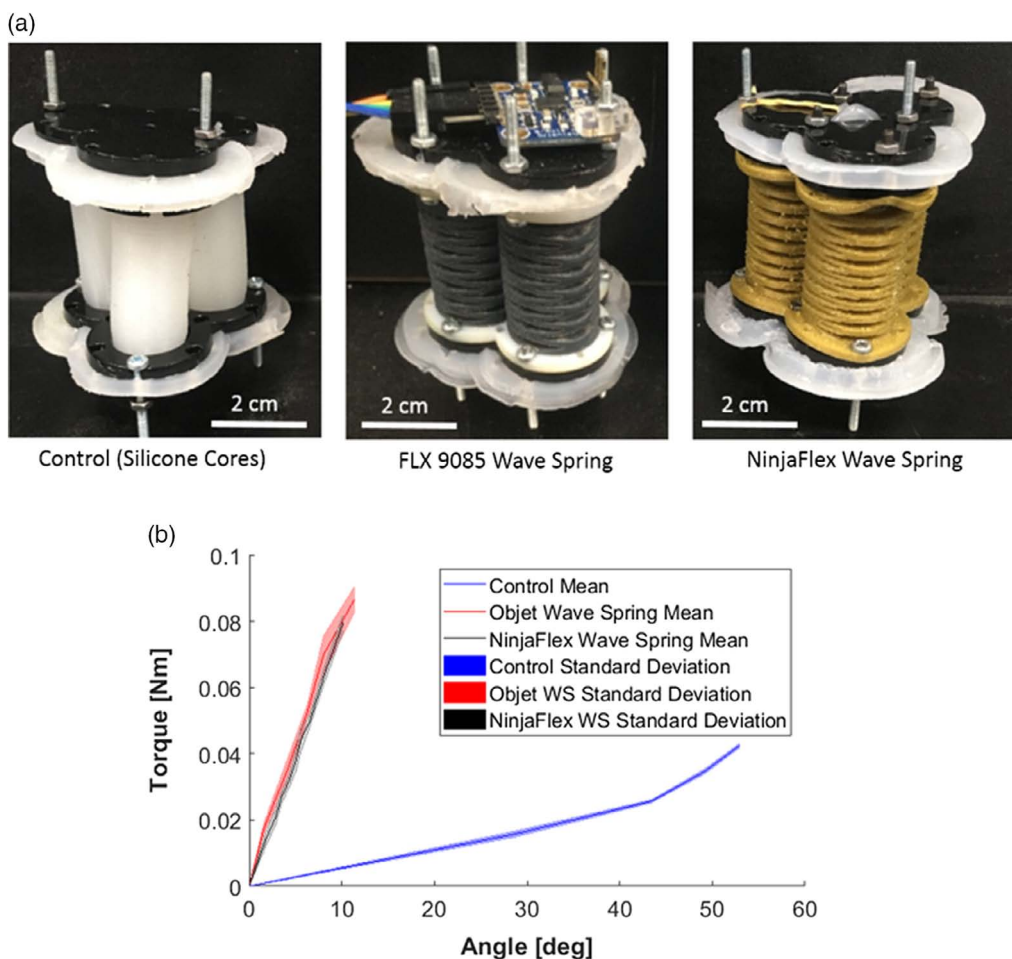


**Figure 4.** a) A three-chamber NinjaFlex bending wave spring actuator (left) along with the silicone pressure chambers alone (right). b) Results of a torsion test comparing the torsional stiffness of three-chamber wave spring bending segments with the silicone cores on their own. There was minimal difference between the two materials tested, both of which exhibited ten times the stiffness of the control.

represented approximately half the height of a layer. Although we could also change the period of each wave continuously, it was necessary for the period to be a multiple of the perimeter of the wave spring (which we held constant), to ensure that the wave connected back to itself.

We examined the effects of changing parameters on the torsional stiffness of the one-chamber wave springs using both physical experiments and finite element analysis (FEA). We used physical experiments to get a wider picture of the design space, whereas FEA was used to drill down with higher resolution on a single number of waves per level. The parameters we chose to investigate with physical experiments were [0.06 0.0675 0.075 0.0825 0.09] in. ([1.524 1.7145 1.905 2.0955 2.286] mm) in amplitude and [3 4 5] waves per level, whereas our FEA focused on five waves per level with amplitudes tested in the same range but with a resolution of 0.0025" (0.0635 mm). We printed a wave spring out of NinjaFlex for each combination and performed torsional tests using the same experimental setup as the previous section. The wave amplitudes that were investigated could not match up exactly with the height of the top layer, and thus differing amounts of partial waves were included at the end to make up

the difference, which were filled in to reduce the risk of the wave spring breaking.

We used the results of these torsion tests to calculate the stiffness of each wave spring. These results are shown in Figure 5b. We found that increasing the number of waves increased the torsional stiffness of the wave spring, as expected. However, we found that the 0.075" amplitude wave springs were the strongest. This went against our hypothesis that a shorter amplitude would be stronger because with a shorter amplitude the loading on the links of the wave would approach column loading. However, our experiments indicated that this was not the case.

We simulated a single layer (such as the one shown in Figure 5a) of the wave spring and multiplied the mean displacement on its upper faces by the number of layers in the entire spring. Simulations were performed in SolidWorks, with material properties taken from the manufacturer.<sup>[31]</sup> Results are shown in Figure 5c, in comparison with the five-layer experimental results. We found general agreement between the FEA and the experimental results. The FEA results do indicate that the stiffness of the 0.075" wave spring was caused by the way that amplitude divided into the total actuator length. Increasing

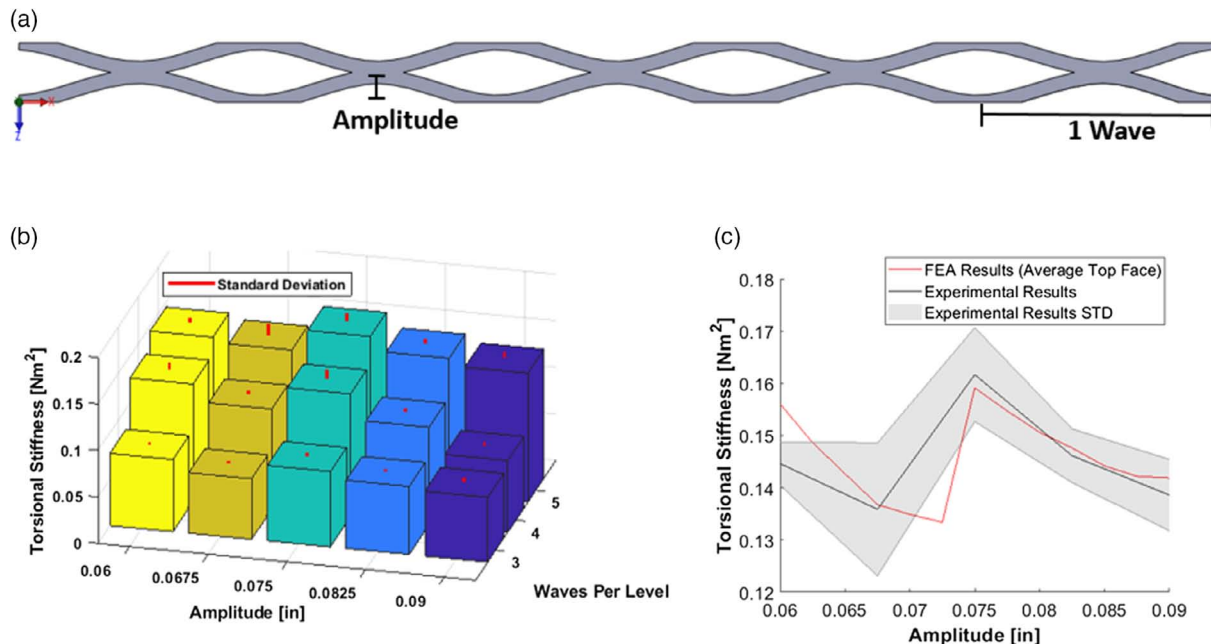


**Figure 5.** a) An unwrapped wave spring layer, showing the parameters investigated. This example had an amplitude of 0.075" (1.905 mm) and five waves per level. In addition, this served as the template for the FEA verification experiments. b) Torsional stiffness results (with standard deviations) for the range of wave spring actuators tested. c) A comparison of the FEA torsional stiffness results with the experimental results for five waves per level, with amplitudes ranging from 1.524 to 2.286 mm.

the amplitude of the waves makes the wave spring weaker, but when the amplitude gets high enough that fewer waves can be fit in the actuator, the stiffness increases again. The amplitude 0.075" was just on the tip of a reduction in number of waves that could fit within the fixed height of the actuator, giving it a higher stiffness. In addition, the lower resolution of physical experiments caused the difference between the FEA and experimental results at 0.0725" with the trend in negative stiffness likely continuing until the jump at 0.075".

Thus, as these interface zone seems to have such a significant impact on the torsional stiffness of these wave springs, we can also conclude that wave amplitude did not have a significant effect for the amplitudes we investigated. Thus, we can use the amplitude that is most beneficial to the application without worrying about reductions in torsional stiffness.

## 4. Three-Segment Manipulator

We expanded this approach of creating wave spring bending modules and created a three-segment manipulator, as shown in Figure 6.

### 4.1. Fabrication

This manipulator was assembled out of three modules similar to the one shown in Figure 4. To fit the pressure lines (three for each segment), the lower bases needed to have a hollow central shaft. To make space, the pressure chambers were shifted outward by 2 mm for the middle segment and 4 mm for the base segment. Finally, an additional wave spring was added in the

center of the lower two segments, connecting to the outer wave springs surrounding the pressure chambers. This increased the torsional stiffness of the segments by linking the three separated wave springs together into a single unit.

Altogether, this results in a sturdy and torsionally stiff manipulator. Some example states, when mounted in an upright or inverted configuration, are shown in Figure 7 with a vacuum suction gripper mounted at the end, where we can see that the manipulator is capable of a wide range of configurations without drooping.

### 4.2. Manipulation Task

These configurations show the general capabilities of the wave spring manipulator, but do not highlight the improvements that the wave springs afford. To do so, we used it to perform a simple pick-and-place task. We mounted it in a cantilever configuration and used it to pickup and drop-off a small weighted cardboard box. Images of this manipulation task are shown in Figure 8a. The cantilever configuration represents the worst-case scenario for continuum manipulation, where the actuator must overcome the most torque around its base.

Pressure in the nine pressure chambers was controlled using pulse-width modulation (PWM) of an array of digital valves connected to a 12.5 psi pressure source, similarly to our previous work<sup>[32]</sup> and others.

These experiments were performed in a motion capture environment, which was used to track the box as it was carried from the pickup to the drop-off locations. Trajectories from some of these experiments are shown in Figure 8b. The most variation in the manipulator behavior occurred when it extended to pick

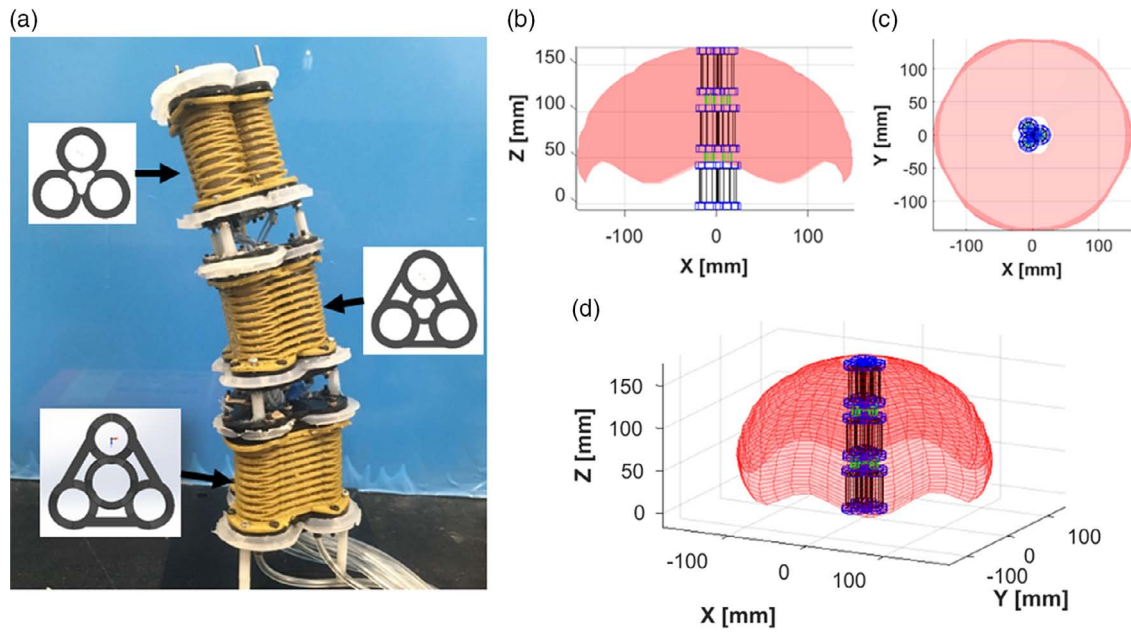


**Figure 6.** We created a manipulator using three of the three-chamber wave spring actuators mounted in series. The wave springs were printed out of NinjaFlex, with the lower segments being slightly wider in order to accommodate the pressure lines. a) The physical system with insets indicating the sections' cross sections, with horizontal supports and an additional wave spring inserted in the lower two segments to improve stiffness while giving space for the pressure lines. b–d) An approximation of the workspace of the manipulator from various angles. This was calculated using continuum manipulator kinematics discussed in Santoso et al.<sup>[12]</sup> Because of the three-chamber construction of the manipulator, the workspace is not a perfect dome.

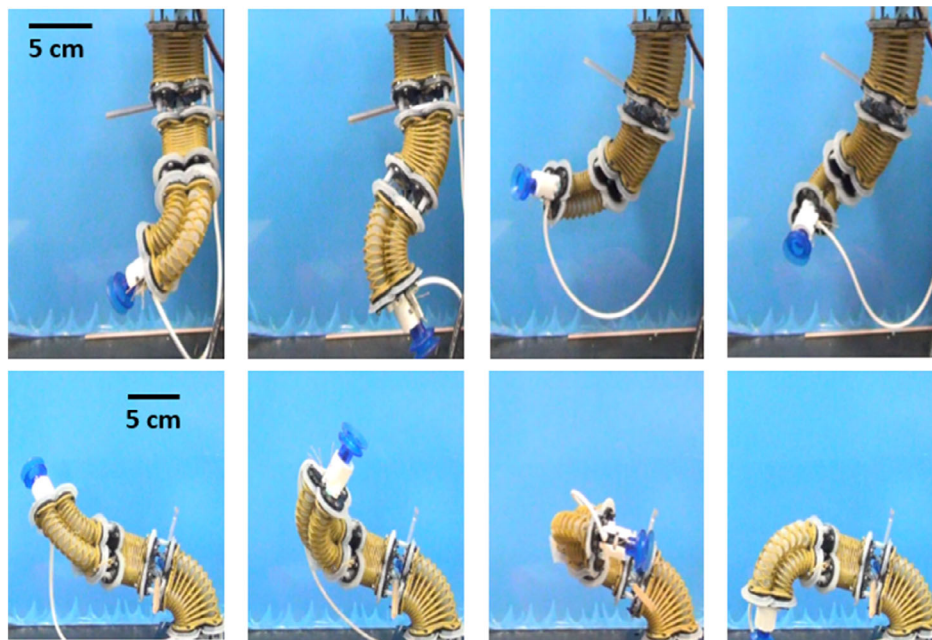


**Figure 7.** A range of states that the manipulator is capable of.

up the box. This, combined with slight difference in box placement, resulted in the suction gripper grasping the box in different places. This resulted in the offsets between box trajectories shown.

To quantify the usefulness of the wave springs, we calculated the axial torque from the tip segment and payload on the base

segment to be around 170 N mm. Using torsional stiffness data of a more traditional continuum manipulator of similar size, the soft snake segments used in our earlier work,<sup>[33]</sup> we calculated that such a base segment would have twisted 55°, enough to prevent the payload from being lifted off the ground entirely.

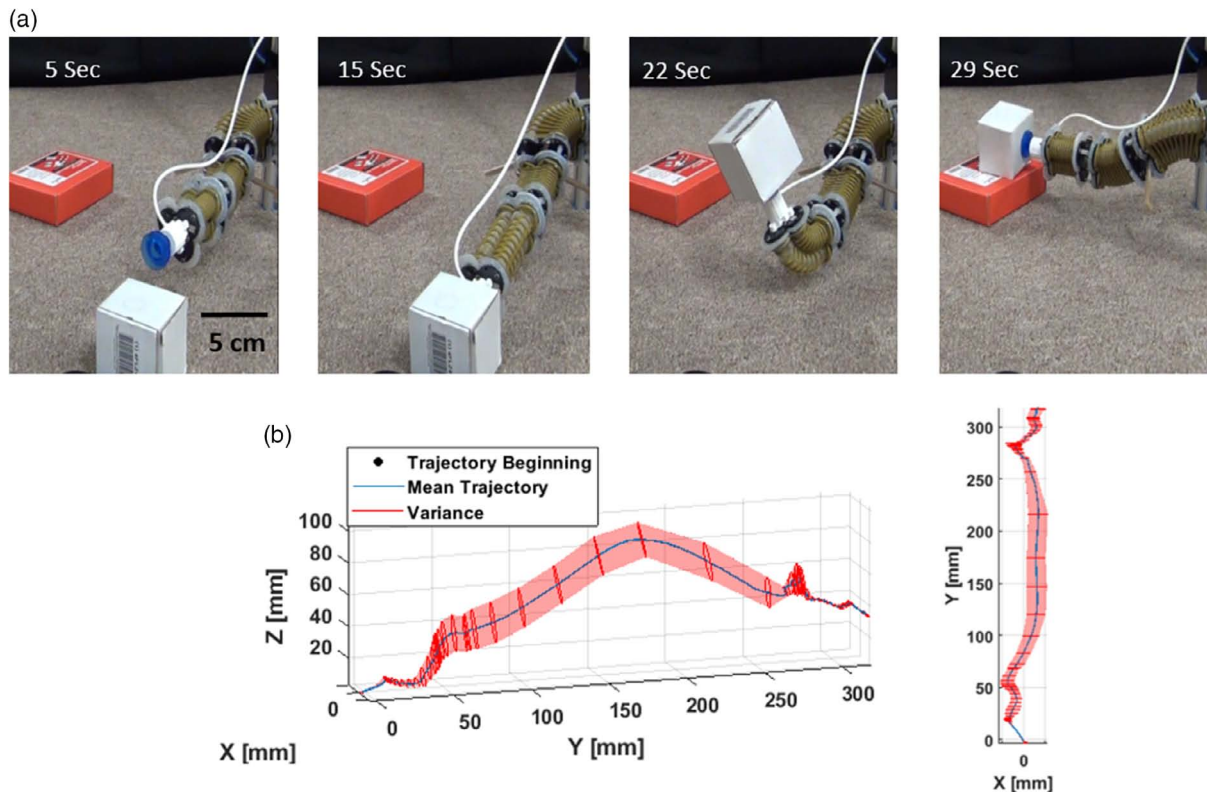


**Figure 8.** a) Images from the wave spring manipulator pick-and-place experiment. b) The trajectories of the object moved by the manipulator during several trials. Maximum variance is 1.6 cm.

This represents a proof of concept for the advantages that flexible wave springs can bring to continuum manipulators.

## 5. Conclusion

This article discussed a new paradigm in soft pneumatic actuator design. This paradigm combines traditional silicone molding with flexible 3D printed wave springs to create actuators that are soft and flexible while exhibiting a high torsional stiffness. We performed initial investigations of single- and three-chamber wave spring actuators and found that they vastly improved torsional stiffness of soft pneumatic actuators. We investigated changing the amplitude and number of waves per level of single-chamber soft actuators through both experimentation and FEA. We found that the more the waves per level the higher the torsional stiffness, but that changing the amplitude of each wave did not significantly impact the torsional stiffness overall. Finally, we combined these individual three-chamber wave spring actuators into a nine-DoF bending manipulator, which we used to perform a pick-and-place task in an anticancer configuration that would have been much more difficult or even impossible for a traditional bending manipulator with a lower torsional stiffness. This represents the first time torsional stiffness has been demonstrated in a soft pneumatic continuum manipulator.

One weakness with the hybrid manipulator demonstrated in this article is its lack of active strength when compared with some of the other continuum manipulators in the literature,

particularly the Octarm.<sup>[1]</sup> The manipulator we used was a proof-of-concept for the hybrid continuum design, with little effort made toward increasing the force outputs to levels that would allow for practical applications. This could be done using larger pressure chambers, which would allow the manipulator to apply greater forces. Using threading or a tighter mesh around the pressure chambers would also increase output forces by allowing the pressure chambers to withstand higher pressures without bursting and reducing the necessary wall thickness. Although the inclusion of the wave spring sheath allows the soft linear actuator to function without the need for constrain threading, it did not work perfectly. The required thickness of the 3D printed wave springs means that they cannot be packed tightly enough to keep the silicone actuators from bursting at high pressure. Dynamic performance could be increased using a wider pressure lines or a larger valve, which would increase the flow rate of pressure into the actuator chambers.

Alternately, work could be done to reduce the weight of the bending segments, so that a smaller percentage of the force output needs to be devoted to countering the effects of gravity on the manipulator, itself. In addition, as the wave spring sheathes do not have to obstruct the inner workings of a continuum actuator, they can be combined with other controllable stiffness techniques discussed in Section 1 to create an even more capable manipulator.

We used a wave spring manipulator to perform a pick-and-place task, but the pressures used were determined by hand. Important future work includes creating a model of the soft

continuum manipulator under load and using it to perform accurate inverse kinematics, as well as control algorithms that would allow the manipulator to reliably reach desired points. This would allow the soft wave spring continuum manipulator to operate as a robotic limb, easily performing tasks in complex unstructured environments without risk and allow for humans and robots to share the same environments and collaborate on the same tasks.

## Acknowledgements

This material was based upon work partially supported by the National Science Foundation (NSF) under award nos. CMMI-1728412 and CMMI-1752195. Any opinions, findings, and conclusions or recommendations expressed in this material are those of the authors and do not necessarily reflect the views of the NSF. The authors thank Raagini Rameshwar and Sarah Schultz for help with the manuscript.

## Conflict of Interest

The authors declare no conflict of interest.

## Keywords

pneumatic actuators, soft robotics, 3D printing

Received: August 8, 2019

Revised: September 19, 2019

Published online: November 4, 2019

- [1] W. McMahan, V. Chitrakaran, M. Csencsits, D. Dawson, I. D. Walker, B. A. Jones, M. Pritts, D. Dienno, M. Grissom, C. D. Rahn, in Proc. IEEE Int. Conf. on Robotics and Automation, ICRA (Ed: S. Hutchinson), IEEE, Orlando, FL **2006**, pp. 2336–2341.
- [2] G. Gerboni, T. Ranzani, A. Diodato, G. Ciuti, M. Cianchetti, A. Menciassi, *Meccanica* **2015**, *50*, 2865.
- [3] K. Zhang, C. Qiu, J. S. Dai, *J. Mech. Robot.* **2016**, *8*, 0310010.
- [4] W. McMahan, B. A. Jones, I. D. Walker, in IEEE/RSJ Int. Conf. on Intelligent Robots and Systems (Eds: M. Meng, H. Zhang), IEEE, Edmonton **2005**, pp. 2578–2585.
- [5] D. C. Rucker, R. J. Webster III, *IEEE Trans. Robot.* **2011**, *27*, 1033.
- [6] A. Loeve, P. Breedveld, J. Dankelman, *IEEE Pulse* **2010**, *1*, 26.
- [7] M. Cianchetti, T. Ranzani, G. Gerboni, T. Nanayakkara, K. Althoefer, P. Dasgupta, A. Menciassi, *Soft Robot.* **2014**, *1*, 122.
- [8] M. S. Moses, M. D. M. Kutzer, H. Ma, M. Armand, in IEEE Int. Conf. on Robotics and Automation (Ed: L. Parker), IEEE, Karlsruhe, Germany **2013**, pp. 4008–4015.
- [9] A. Jiang, A. Ataollahi, K. Althoefer, P. Dasgupta, T. Nanayakkara, in 36th Mechanisms and Robotics Conf., Parts A and B, Vol. 4, (Eds: C. A. Nelson, J. S. Dai), ASME, New York, NY **2012**, pp. 267–275.
- [10] F. Alambeigi, R. Seifabadi, M. Armand, in *IEEE Int. Conf. on Robotics and Automation (ICRA)* (Ed: A. Okamura), IEEE, Stockholm **2016**, pp. 758–764.
- [11] S. M. H. Sadati, L. Sullivan, I. D. Walker, K. Althoefer, T. Nanayakkara, *IEEE Robot. Autom. Lett.* **2018**, *3*, 2283.
- [12] J. Santoso, E. H. Skorina, M. Luo, R. Yan, C. D. Onal, in IEEE/RSJ Int. Conf. on Intelligent Robots and Systems (IROS) (Eds: H. Zhang, R. Vaughan), IEEE, Vancouver **2017**, pp. 2098–2104.
- [13] L. Paez, G. Agarwal, J. Piak, *Soft Robot.* **2016**, *3*, 11.
- [14] P. Qi, C. Qiu, H. Liu, J. S. Dai, L. D. Seneviratne, K. Althoefer, *IEEE/ASME Trans. Mechatronics* **2016**, *21*, 1281.
- [15] C. D. Onal, M. T. Tolley, R. J. Wood, D. Rus, *IEEE/ASME Trans. Mechatronics* **2015**, *20*, 2214.
- [16] R. J. Murphy, M. D. M. Kutzer, S. M. Segreti, B. C. Lucas, M. Armand, *Robotica* **2014**, *32*, 835.
- [17] K. Xu, M. Fu, J. Zhao, in IEEE Int. Conf. on Robotics and Automation (ICRA) (Ed: L. Parker), IEEE, Hong Kong **2014**, pp. 3258–3264.
- [18] E. H. Skorina, M. Luo, S. Ozel, F. Chen, W. Tao, C. D. Onal, in IEEE Int. Conf. on Robotics and Automation (ICRA) (Ed: A. Okamura), IEEE, Seattle, WA **2015**, pp. 2544–2549.
- [19] M. Luo, E. H. Skorina, W. Tao, F. Chen, C. D. Onal, in Int. Conf. on Technologies for Practical Robot Applications (TePRA) (Ed: H. Greiner), IEEE, Woburn, MA **2015**.
- [20] E. H. Skorina, M. Luo, W. Y. Oo, W. Tao, F. Chen, S. Youssefian, N. Rahbar, C. D. Onal, *PLoS One* **2018**, *13*, 1.
- [21] G. K. Klute, J. M. Czerniecki, B. Hannaford, in IEEE/ASME Int. Conf. on Advanced Intelligent Mechatronics (Eds: K.-M. Lee, B. Siciliano), IEEE, Atlanta, GA **1999**, pp. 221–226.
- [22] R. H. Gaylord, *US Patent 2844126*, **1958**.
- [23] M. Luo, Y. Pan, E. Skorina, W. Tao, F. Chen, S. Ozel, C. Onal, *Bioinspiration Biomimetics* **2015**, *10*, 055001.
- [24] B. N. Peele, T. Wallin, H. Zhao, R. F. Shepherd, *Bioinspiration Biomimetics* **2015**, *10*, 055003.
- [25] H. K. Yap, H. Y. Ng, C.-H. Yeow, *Soft Robot.* **2016**, *3*, 144.
- [26] Y. Yang, Y. Chen, *IEEE Robot. Autom. Lett.* **2018**, *3*, 656.
- [27] Y. Mori, M. Zhu, H. Kim, A. Wada, M. Mitsuzuka, Y. Tajitsu, S. Kawamura, in IEEE/RSJ Int. Conf. on Intelligent Robots and Systems (IROS) (Eds: C. Balaguer, C. Laschi), IEEE, Madrid **2018**, pp. 5952–5957.
- [28] O. D. Yirmibesoglu, J. Morrow, S. Walker, W. Gosrich, R. Caizares, H. Kim, U. Daalkhajav, C. Fleming, C. Branyan, Y. Menguc, in 2018 IEEE Int. Conf. on Soft Robotics (RoboSoft) (Eds: C. Laschi, F. Iida), IEEE, Livorno **2018**, pp. 295–302.
- [29] J. Plott, X. Tian, A. J. Shih, *Addit. Manuf.* **2018**, *22*, 606.
- [30] C. Yuan, D. J. Roach, C. K. Dunn, Q. Mu, X. Kuang, C. M. Yakacki, T. J. Wang, K. Yu, H. J. Qi, *Soft Matter* **2017**, *13*, 5558.
- [31] NinjaTek Technical Specifications, <https://ninjatek.fppsites.com/wp-content/uploads/2018/10/NinjaFlex-TDS.pdf> (accessed: June 2019).
- [32] E. Skorina, W. Tao, F. Chen, M. Luo, C. D. Onal, in IEEE Int. Conf. on Robotics and Automation (ICRA) (Ed: A. Okamura), IEEE, Stockholm **2016**.
- [33] Y. Qin, Z. Wan, Y. Sun, E. H. Skorina, M. Luo, C. D. Onal, in IEEE Int. Conf. on Soft Robotics (RoboSoft) (Eds: C. Laschi, F. Iida), IEEE, Livorno **2018**, pp. 77–82.